Biophysical Chemistry 137 (2008) 7–12

Contents lists available at ScienceDirect

Biophysical Chemistry

journal homepage: http://www.elsevier.com/locate/biophyschem

Softening of POPC membranes by magainin

Hélène Bouvrais [a,b], Philippe Méléard [b], Tanja Pott [b], Knud J. Jensen [c], Jesper Brask [c], John H. Ipsen [a,*]

[a] Department of Physics and Chemistry, MEMPHYS-Center for Biomembrane Physics, University of Southern Denmark, Odense, Denmark
[b] UMR-CNRS 6510, Université de Rennes 1, Rennes, France
[c] Department of Natural Sciences, Section for Bioorganic Chemistry, University of Copenhagen, Frederiksberg, Denmark

ARTICLE INFO

Article history:
Received 28 March 2008
Received in revised form 2 June 2008
Accepted 2 June 2008
Available online 17 June 2008

Keywords:
Lipid bilayer
Vesicle fluctuation analysis
Membrane mechanics
Magainin
Bending elasticity
Continuum model

ABSTRACT

Magainin 2 belongs to the family of peptides, which interacts with the lipid membranes. The present work deals with the effect of this peptide on the mechanical properties of 1-palmitoyl-2-oleoyl-*sn*-glycerol-3-phosphocholine Giant Unilamellar Vesicle, characterized by the bending stiffness modulus. The bending elastic modulus is measured by Vesicle Fluctuation Analysis at biologically relevant pH and physiological buffer conditions and shows a dramatic decrease with increasing peptide concentration. The observed bilayer softening is interpreted in terms of a continuum model describing perturbations on the membrane organization. Our analysis suggests that the adsorbed peptides give rise to considerable local curvature disruptions of the membrane.

1. Introduction

Since their discovery 20 years ago as components of the innate immune system of the African clawed frogs *Xenopus laevis* [1], magainins have been subject to intensive biophysical studies as model systems for the understanding of the interactions between antimicrobial peptides and biomembranes. Membranes are the likely target for the magainin actions because these peptides display a relatively unspecific and broadband antimicrobial activity [2] probably due to their amphipatic nature. More specifically, magainin 2 and its synthetic derivatives have been scrutinized. Magainin 2 consists of 23 amino acids with a net positive charge z=+4 [3] under physiological conditions (z=3.6–3.8 for the magainin 2-amide [4]). Numerous studies support the picture that magainins exhibit a random coil conformation in solution [5–7]. Adsorbed on membranes, they fold as α-helices lying parallel on the bilayer surface, their hydrophobic residues being buried into one of the monolayers of the lipid bilayer structure [5–15]. At low adsorbed peptide densities, the helices are relatively spread on the surfaces [16], while at higher membrane concentrations, pore-like structures resulting from the aggregation of transmembrane oriented peptides have been shown on oriented lipid bilayers by X-ray, circular dichroism and NMR studies [15,17]. These properties are common to a variety of antimicrobial peptides including melittins, cecropins and ovispirins [18].

The precise mode of actions for the antimicrobial activity of magainin and similar antimicrobial peptides is still unclear. However, the observed membrane lytic activity on biological membranes and the pore forming ability of magainin in model membranes [19,20] have focussed the attention on models where magainins break down the barrier properties of the membrane. In particular, different models of pores through the membranes have been popular for the magainin, like the transmembrane helical bundles (analogous to the barrel stave model for the alamethicin) [21,22], the toroidal model [3,19], the carpet model [23,24] and the detergent like peptide model [25,26], for review see [27,28]. It has been challenging to prove that the antimicrobial action is linked to any of these models. Further, it is complicating the matter that the models are not mutually exclusive and may be applicable at different system conditions. For magainin, it is clear that the membrane barrier capacity is reduced by the presence of peptides in the membrane, while the data cannot support the formation of well-defined membrane channels.

In the present study, we have demonstrated that another material property of the membrane, the bending rigidity, is severely affected by the presence of magainin 2. By analysis of the flicker spectrum of Giant Unilamellar Vesicles (GUVs) under physiological buffer conditions, we show that the bending rigidity of POPC vesicles is dramatically reduced at μM bulk concentrations of magainin 2. Furthermore, by use of a model interpretation of the data in terms of a continuum description of the membrane, we gain important information about model parameters and the local and global effects of the peptide insertions into a membrane. This work represents to our knowledge the first material characterization of GUVs under physiological buffer conditions.

The paper is organized as follows. In Materials and methods section, the peptide synthesis, the GUVs preparation under physiological buffer conditions and the technique of Vesicle Fluctuation

* Corresponding author.
E-mail address: ipsen@memphys.sdu.dk (J.H. Ipsen).

0301-4622/$ – see front matter © 2008 Elsevier B.V. All rights reserved.
doi:10.1016/j.bpc.2008.06.004

Analysis (VFA) are presented. In the section Results and discussion, the data from the measurements of the bending rigidity are given and discussed, the effects of partitioning and electrostatics are treated and applied to our results. Finally, the data are interpreted in terms of a minimal continuum model describing the effects of peripheral peptides inclusions on membrane bending elasticity.

2. Materials and methods

2.1. Synthesis of magainin 2

Magainin 2 was prepared by automated solid-phase peptide synthesis (SPPS) using Fmoc(9-fluorenylmethyloxycarbonyl)-amino acids. Amino acid symbols denote the L-configuration unless stated otherwise. All solvent ratios are volume/volume unless stated otherwise.

NovaSyn TG (Tentagel) resin and Fmoc-amino acids for peptide synthesis were from Novabiochem (Läufelfingen, Switzerland), HBTU (*N* -[(1*H* -benzotriazol-1-yl) (dimethylamino)methylene]-*N* -methylmethanaminium hexafluorophos-phate *N*-oxide) and HOBt (1-hydroxybenzotriazole) were from IRIS Biotech, while all other commercial compounds were purchased from Sigma-Aldrich (Copenhagen, Denmark). ESI-MS spectra were obtained on a Micromass LCT instrument (MassLynx software) by direct injection of an aqueous solution of the lyophilized product. HPLC analyses were carried out on a Waters system (600 control units, 996 PDA detectors, 717 Plus autosamplers, Millennium32 control software) equipped with either a Waters Symmetry300 C_{18} 5 µm column or a Waters Symmetry300 C_4 5 µm column, both 3.9×150 mm. Preparative HPLC was carried out on a similar Waters system (with a Delta 600 pump) equipped either with a stack of three 40×100 mm column cartridges of Waters Prep Nova-Pak HR C_{18} 6 µm 60 Å, or with a single 25×100 mm column cartridge of Waters Delta-Pak HR C_4 15 µm 300 Å. Magainin 2 was eluted with mixtures of CH_3CN and H_2O, both containing 0.1% TFA (trifluoroacetic acid).

The magainin 2 sequence, H-Gly-Ile-Gly-Lys-Phe-Leu-His-Ser-Ala-Lys-Lys-Phe-Gly-Lys-Ala-Phe-Val-Gly-Glu-Ile-Met-Asn-Ser-OH, was assembled using a MilliGen 9050 PepSynthesizer starting with a FmocSer(tBu)-Tentagel (NovaSyn TG resin, 0.50 g, 0.16 mol/g). Amino acids were coupled as their N^{α}-Fmoc protected derivatives; the following trifunctional amino acid derivatives were used: Fmoc-Ser (tBu)-OH, Fmoc-Glu(*t*Bu)-OH, Fmoc-Lys(Boc)-OH, Fmoc-Asn(Trt)-OH and Fmoc-His(Trt)-OH. For each activation (coupling) step, 4 eq of Fmoc-amino acids, 3.8 eq of HBTU, 4 eq of HOBt and 8 eq of DIPEA (*N*, *N*′-diisopropylethylamine) were coupled for 30 min. However, Asn, Val and His, as well as the amino acids following these, were coupled for 60 min. Finally, the peptide was cleaved off with Reagent K, TFA-PheOH-H_2O-$PhSCH_3$-EDT (82.5:5:5:5:2.5, 8 mL) for 1 h. The resin was filtered and washed with TFA (3×5 mL), and the combined cleavage-mixture and washings were concentrated to 2 mL, and precipitated with cold diethyl ether (35 mL). After centrifugation, the pellet was redisolved in TFA (2 mL) and re-precipitated with cold diethyl ether (35 mL), which was repeated twice. The precipitate was dissolved in H_2O–CH_3CN (1:1, 10 mL) and was purified by preparative C_{18} RP-HPLC to give magainin 2 as a white powder after lyophilization. Yield 79 mg; ~31% (included 6×TFA). ESI-MS, calculated for C_{114} H_{180} N_{30} O_{29} S_1: 2466.95 Da. Found: *m*/*z* 1234.08 $[M+2H]^{2+}$, 823.22 $[M+3H]^{3+}$, 617.64 $[M+4H]^{4+}$.

2.2. Preparation of giant vesicles under physiological conditions

POPC (1-palmitoyl-2-oleyl-*sn*-glycerol-3-phosphocholine) (purity>98%) was obtained from Avanti Polar Lipids Inc. (Birmingham, Alabama, USA). Some MilliQ Water (Millipore, Bedford MA, USA) were added to the POPC powder to obtain a lipid concentration of about 0.2 mg/mL. The dispersion was agitated gently and the lipids hydrated for a few minutes. Then the dispersion was sonicated in order to obtain SUVs. For that step, a sonicator (Misonix sonicator 3000) was used: five sonications of two minutes were made at 70 W, with a break of five minutes between each sonication so that there was not too much heat transferred in the sample. The sonicated dispersion was filtered using a 0.2 µm filter (sterile celluloseacetate membrane) to remove metal particles.

SUVs deposits were made on platinum wire electrodes (6 spots of 1.5 µL on each electrode) using the sonicated dispersion prepared as previously described. The water was evaporated during several hours and during this step the electrodes were protected from the light. When the water has been evaporated, the electrodes were immersed in a magainin solution of high salinity: 100 mM of NaCl (sodium chloride) in order to be under conditions similar to the physiological ones, 10 mM of Tris (2-amino-2-hydroxymethyl-1,3-propanediol) adjusted to pH≈7.4 and 2 mM of EDTA (ethylenediamine tetraacetic acid). NaCl (purity>99.5%) was obtained from Fluka, Tris (ultra pure product) from Research Organics and EDTA (purity>99.4%) from Sigma-Aldrich (Denmark). This buffer solution with varied concentrations of magainin was introduced in cells made of optical glass (Hellma), with a light path of 1 mm. The GUVs were formed by electroformation, but the standard protocol typically used for water or low-salt environments [29,30] was modified in order to obtain giant vesicles under physiological buffer conditions [31]. The big difference with the standard protocol was the frequency used during the electroformation, that is to say 500 Hz instead of 10 Hz. When the electrodes were connected, an electric field of 150 mV at 500 Hz was applied during 10 min by using a waveform generator (Agilent 33120A 15 MHz function). Then, the electric field at 500 Hz was increased until 1.35 V during 20 min and finally the electric field was pushed to 3.9 V for 90 min. Big vesicles with a diameter between 5 and 50 µm were visible on the electrodes. At the end, both the frequency and the amplitude of the electric field were decreased to respectively 3 Hz and 1 V for 30 min in order to facilitate the removal of the vesicles from the electrodes.

2.3. Vesicle fluctuation analysis

Vesicles were observed directly in the electroformation cuvette, which was placed in a home custom made temperature controlled chamber holder (30 °C). Vesicles were visualized using a phase contrast microscope (Axiovert S100 Zeiss, Göttingen, Germany), equipped with a ×40/0.60 objective (440865 LD Achroplan) and a magnification lens. The vesicle two-dimensional contour in the focal plane of the objective was thus obtained. A CCD Camera (SONY SSC-DC50AP) was used to capture a series of 3000 to 4000 contours in real time at a rate of 25 frames per second with a video integration time of 4 ms. Using home custom made software, the bending elastic modulus was obtained for a given system as an average of 10 to 30 vesicles with a diameter between 5 and 30 µm.

Vesicle fluctuation analysis was the technique used to determine the bending elastic modulus of POPC/magainin 2 systems. Values of the bending elasticity were extracted from thermally induced shape undulations of the membrane. The shape of an homogeneous lipid bilayer is described by Helfrich's curvature free energy [32]:

$$F = \frac{\kappa}{2}\int_A dA \cdot \left(\frac{1}{r_1}+\frac{1}{r_2}-2H_0\right)^2 \quad (1)$$

where r_1 and r_2 are local curvature radii, and κ is the bending elastic modulus; H_0 is the spontaneous curvature of the membrane, which reflects asymmetry in the composition of the two monolayer leaflets of the membrane. Due to the procedure used to form giant vesicles, we assume a complete symmetry in both monolayers, therefore $H_0=0$.

For each captured frame, the center of mass and the instantaneous vesicle contour in the focal plane are obtained and then the contour

shape is characterized in polar coordinates $r(\phi, t)$. To quantify the shape thermal fluctuations, the angular correlation function of the relative radius fluctuations is calculated [33]:

$$\xi(\psi,t)=\frac{1}{R^2}\left(\left(\frac{1}{2\pi}\int_0^{2\pi} d\phi\cdot r(\phi+\psi,t)\cdot r(\phi,t)\right)-\left(\frac{1}{2\pi}\int_0^{2\pi} d\phi\cdot r(\phi,t)\right)^2\right) \quad (2)$$

where R is the average radius of the contour.

By expanding $\xi(\psi, t)$ using Legendre polynomials $P_n(\cos\psi)$ ($\xi(\psi,t)=\Sigma_n B_n(t).P_n(\cos\psi)$, $n\geq 2$) and making time average of the amplitudes in the Legendre expansion $\langle B_n\rangle_t$, the spectrum of the shape fluctuations of the quasi-spherical vesicle is then obtained. The average of all coefficients, $\langle B_n\rangle_t$, is thus fit to a theoretical expression for the Legendre amplitudes:

$$\langle B_n(\kappa,\overline{\sigma})\rangle=\frac{k_BT}{4\pi\kappa}\frac{2n+1}{(n+2)(n-1)(\overline{\sigma}+n(n+1))} \quad (3)$$

where $n\geq 2$. Here n is the Legendre mode number and, κ and $\bar{\sigma}$ are fitting parameters obtained by a χ^2-fit of the Eq. (3). $\bar{\sigma}$ reflects the amount of surface excess area for the vesicle and is thus varying strongly between the vesicles.

Vesicles were selected when $\chi^2_{\min}\approx f$, where $f=n_{\max}-n_{\min}$ is the number of degrees of freedom for the χ^2-fit, and when κ and $\bar{\sigma}$ were not excessively large. $n_{\min}$ and $n_{\max}$ are the lowest and highest modes to be considered in the analysis [34]. High κ values may indicate a multilamellar vesicle, while very large $\bar{\sigma}$ values signal a tense membrane which may distort the analysis.

An alternative method in order to obtain the bending rigidity is the micropipette technique, where the low tension entropic elasticity yields information about the bending elastic modulus [35,37]. However for membranes with partitioning agents, the vesicle fluctuations technique is superior, since an applied tension severely perturbs the partitioning into a membrane.

3. Results and discussion

In this section, we will present and discuss the decrease in the observed bending rigidity of POPC-membranes in presence of magainin 2 and interpret the results in terms of membrane partitioning of magainin and its effects on the thermo-elasticity of bilayer membranes.

3.1. Magainin effects on the bending elasticity

In this study, we investigate the physical perturbations induced by magainin 2 on the membrane. For that purpose the bending elasticity, κ, is a key parameter to describe membrane mechanical properties. The measurements of the bending elastic modulus made at 30 °C for each magainin concentration C_p^t allow us to see peptide effects on the membrane stability. The obtained κ values are displayed in Table 1. The value of κ without magainin is similar to the one obtained by Kučerka et al. with the X-Ray technique also for POPC bilayer, which was equal to 0.85×10^{-19} J [36].

Table 1
Effects of magainin 2 on POPC membranes at 30 °C

C_p^t [μM]	κ [k_BT]
0	24.0±0.3
0.10	20.5±0.9
0.21	15.6±0.3
0.35	12.6±0.5
0.69	9.2±0.5
3.43	5.6±0.3

Values of membrane bending rigidity, κ, were measured by flicker analysis. Error on κ represents standard deviation from the mean value of a vesicle population.

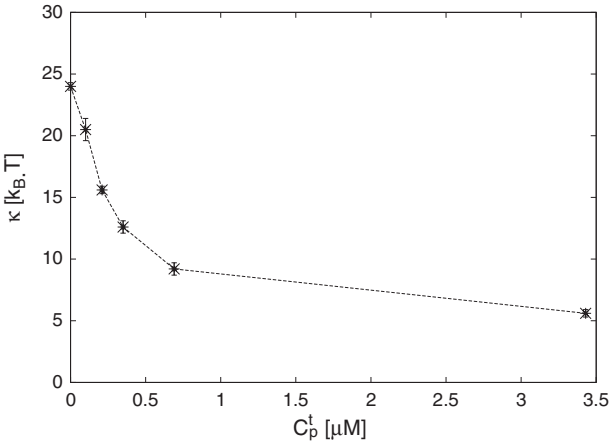

Fig. 1. Experimental decrease of the bending elasticity κ as a function of the magainin 2 concentrations C_p^t. The measurements were made at 30 °C.

In Fig. 1, we clearly see the decrease of the bending rigidity κ as a function of the total peptide concentration C_p^t. A decrease in the bending rigidity of lipid membranes at low peptide levels in pure water has also been reported for alamethicin from the fungus *Trichoderma viride* and for mellitin from the venom of the honey bee *Apis mellifera* [38,39]. This may indicate that the decrease in membrane rigidity is a characteristic of the interactions between membranes and these biomolecules.

It is noteworthy that the dramatic effects on membrane mechanical behavior observed here occur for very low peptide concentrations (micromolar range). Besides, this decrease of the bending rigidity indicates that the peptides cause a softening of the membrane bending resistance.

3.2. Partition coefficient influence

Our results for κ are plotted as a function of total concentrations of peptides (Fig. 1). But, the effects observed on the membranes mechanical properties are induced by the peptides bound to the lipid bilayers. Therefore the interesting concentration is that of the bound peptide, C_p^b. In order to know the C_p^b values, we need the partition coefficient K_p, which is defined according to:

$$\frac{C_p^b}{C_l}=K_p\cdot C_p^M \quad (4)$$

where C_p^M is the peptide concentration close to the membrane and C_l the lipid concentration of the samples.

Consequently, the peptide area coverage AC_p, parameter we choose in order to represent our experimental data, can be written:

$$AC_p=\frac{A_p^b}{A_{\text{memb}}}\approx\frac{A_p^b}{A_l}=\frac{C_p^b\cdot a_p}{C_l\cdot a_l}=\frac{K_p\cdot C_p^M\cdot a_p}{a_l} \quad (5)$$

where a_p and a_l are respectively the cross sectional area per peptide and per lipid equal to 340 Å^2 for the magainin 2 [17,40] and equal to 64 Å^2 for POPC [41].

Using a partitioning study previously published by Wieprecht et al., we can evaluate the peptide area coverage AC_p (Table 2) from their determined partition coefficient of magainin for POPC SUVs in buffer (10 mM Tris and 100 mM NaCl) at 30 °C equal to 2000 M^{-1} [42]. K_p was measured using the technique of isothermal titration calorimetry (ITC). The application of K_p value obtained from SUVs study is based on the observation that partition of amphipatic helices is similar for large and small vesicles [4,43].

Then using electrostatic calculations based on Gouy–Chapman theory, we have determined the C_p^M concentrations for each C_p^t one involved [42]. Thus, we can correlate the C_p^t concentrations to AC_p

Table 2
Correlation between the concentrations of magainin C_p^t and $C_p^M$and the magainin area coverage percentages of the membranes AC_p

C_p^t [μM]	C_p^M[μM]	AC_p [%]
0	0	0
0.10	0.096	0.102
0.21	0.193	0.205
0.35	0.307	0.326
0.69	0.546	0.580
3.43	1.677	1.782

percentages (Table 2). For the first concentrations, the differences between the C_p^Mconcentrations and the C_p^t ones are not so important, because we are in presence of zwitterionic POPC membranes, very low magainin concentrations and buffer solutions of high salinity leading to a maximum Debye length $l_D \sim 10$ Å, if we consider only the contribution of NaCl (screening effect). But, for the highest concentration, a major difference is noted due to the peptide adsorption on the membranes, leading to electric double layer effects.

Now, the bending elastic modulus κ can be plotted as a function of the peptide area coverage AC_p (Fig. 2). It appears thus clearly that magainin 2 effects on the bending rigidity are important for AC_p percentages inferior to 0.5%, corresponding to a big decrease of κ and for higher AC_p percentages, the magainin inclusions effects on κ seem to be less important, leading to a stabilization of the κ values.

3.3. Data modeling

In this part, we will present a simple continuum model describing the effects of peripheral inclusions on membrane stability. It will account for the presence of inclusions in the membrane, which will affect the local membrane curvature and induce interactions between inclusions within the same monolayer and from opposite monolayers.

The shape of a simple, symmetric membrane is well described by Helfrich's free energy (Eq. (1)), where $H_0=0$:

$$F_{\text{Helf}} = \frac{\kappa}{2}\int_A dA \cdot \left(\frac{1}{r_1}+\frac{1}{r_2}\right)^2 \tag{6}$$

In the very dilute limit, the distribution of inclusions on a flat membrane is well described by a 2-D ideal gas:

$$\begin{aligned} F^0_{\text{Gas}} &= k_B T \int_A dA \\ &\cdot \left(\rho_{\text{up}} \cdot \left(\ln\left(\rho_{\text{up}} \cdot a^2\right)-1\right) + \rho_{\text{down}} \cdot \left(\ln\left(\rho_{\text{down}} \cdot a^2\right)-1\right)\right) + cst \\ &\approx \int_A dA \cdot \left(2k_B T \cdot \rho_0 \cdot ln(\rho_0 \cdot a^2) + k_B T \cdot \rho_0 \cdot \left(\frac{\Delta\rho}{2\rho_0}\right)^2 + cst\right) \end{aligned} \tag{7}$$

where $\rho_{\text{up}}=\rho_0-\Delta\rho/2$ and $\rho_{\text{down}}=\rho_0+\Delta\rho/2$ are respectively the local densities of peptides on the upper and lower monolayers, and a represents a molecular length scale in the membrane. ρ_0 is the overall average density while $\Delta\rho$ displays local variations around zero, since the two monolayers are symmetric. Eq. (7) is an expansion of F^0_{gas} up to 2nd order in $\Delta\rho/\rho_0$.

The interactions between inclusions are included as the lowest order virial correction to the ideal gas expression Eq. (7). There are two possible contributions:

(1) the in-plane effective interactions between peptides within the monolayers:

$$F^1_{\text{Gas}} = \frac{t}{2}\int_A dA \cdot \left(\rho^2_{\text{up}} + \rho^2_{\text{down}}\right) = t\int_A dA \cdot \left(\rho_0^2 + \left(\frac{\Delta\rho}{2}\right)^2\right) \tag{8}$$

Contributions to interaction parameter t can originate e.g. from the excluded volume effect $t \sim a_{\text{peptide}} \times k_B T$ and from electrostatic interactions $t \sim z^2 \times k_B T \times l_B l_D$, with Bjerrum length $l_B \sim 7$ Å. Both of these contributions are repulsive and suggest $t \approx 10^{-37}$–10^{-38} J.m^2 [44,45].

(2) The intermonolayer effective interactions between peptides:

$$F^2_{\text{Gas}} = s\int_A dA \cdot \rho_{\text{up}} \cdot \rho_{\text{down}} = s\int_A dA \cdot \left(\rho_0^2 - \left(\frac{\Delta\rho}{2}\right)^2\right) \tag{9}$$

The effective interaction strength s between peptides locating on the two monolayer halves may involve electrostatics, Van der Waals forces and lipid packing effects.

There is no additional first virial corrections, which fulfill the up-down symmetry of the bilayer.

The final contribution to the free energy involves the coupling between the local shape of the membrane and the in-plane peptide distribution:

$$F_{\text{Coupling}} = \lambda\int_A dA \cdot \Delta\rho \cdot \left(\frac{1}{r_1}+\frac{1}{r_2}\right) \tag{10}$$

which is the simplest coupling term which respects the up-down symmetry. $\lambda \times \Delta\rho$ can be understood as a local spontaneous curvature. This description of peripheral proteins insertion has previously been applied in the literature [46].

A simple stability analysis of the total free energy, $F=F_{\text{Helf}}+F^0_{\text{Gas}}+F^1_{\text{Gas}}+F^2_{\text{Gas}}+F_{\text{Coupling}}$, reveals that thermo-mechanical stability of the vesicle is affected by the presence of inclusions. An important result relevant for our measurements is that the effective bending rigidity measured by VFA is modified according to:

$$\kappa^{\text{eff}} = \kappa - \frac{4\lambda^2 \cdot \rho_0/k_B T}{1+(t-s)\cdot\rho_0/k_B T} \tag{11}$$

From Eq. (11), it follows that in the very dilute limit $\rho_0 \ll k_B T/(t-s)$, κ^{eff} decreases linearly with the surface concentration ρ_0, where the slope $4\lambda^2/(k_B T)$ yields information about the coupling λ between membrane curvature and the compositional asymmetry $\Delta\rho$ between the monolayers. At higher concentrations $\rho_0 > k_B T/(t-s)$, κ^{eff} behavior will depend on the sign of the expression $(t-s)$. If $(t-s)>0$, κ^{eff} may saturate at a value $4\lambda^2/(t-s)$ lower than κ, while for $(t-s)\leq 0$, κ^{eff} vanishes, destabilizing the vesicle (Fig. 2, insert).

The characteristic experimentally observed dependence of κ^{eff} on the peptide density ρ_0 in the membrane (Fig. 2) can now be

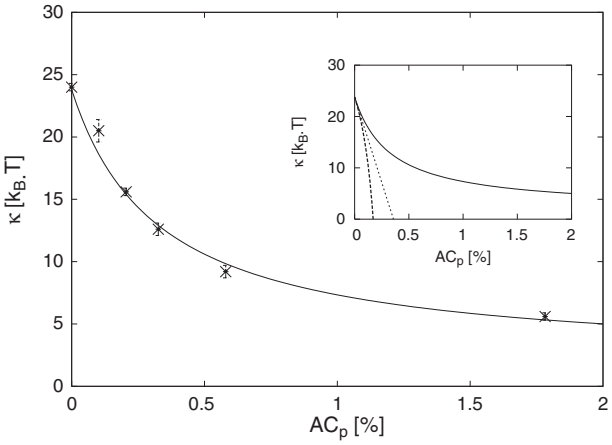

Fig. 2. Comparison between the experimental decrease of the bending elasticity κ at 30 °C as a function of the peptide area coverage AC_p (data point) and a theoretical one (continuous line) for which $\lambda = 3.19 \pm 0.37 \times 10^{-28}$ J·m and $(t-s) = 4.45 \pm 0.09 \times 10^{-36}$ J·m^2. In insert, comparison between different theoretical behaviors of κ for various values of $(t-s)$: continuous line for $(t-s)>0$, dotted line for $(t-s)=0$ and dashed line for $(t-s)<0$.

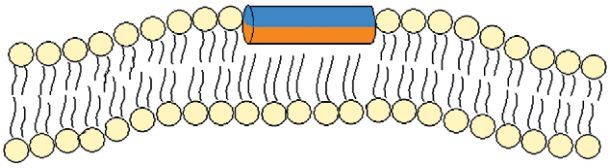

Fig. 3. A cartoon of the effect of a α-helix insertion on the lipid packing.

interpreted from the above model considerations. A fit to Eq. (11) predicts $\lambda = 3.19 \pm 0.37 \times 10^{-28}$ J·m and $(t-s) = 4.45 \pm 0.09 \times 10^{-36}$ J·m^2, shown in Fig. 2. In this dilute range of densities, these estimates are insensitive to the value of a_p.

The obtained value of the coupling parameter λ corresponds to a high local mean curvature, (few nm)$^{-1}$. This leaves a picture of the membrane softening ability of magainin as originating from formation of local, mobile high-curvature spots on the membrane (Fig. 3). Such an estimate of λ due to peripheral inclusions has not been estimated from experimental data before. This coupling constant can in principle be calculated from lipid packing models [44,45].

The observed saturation of κ^{eff} with increasing peptide coverage of the membrane makes the estimate of $(t-s)$ relatively large and positive. Unfortunately, it does not allow for an independent estimate of the two effective inter-peptide interaction parameters. If the in-plane interactions are dominated by contact interactions ($t \sim \pm 10^{-38}$ J·m^2), our estimate suggests significant effective intermonolayer attractive associations $s \sim 10^{-36}$ J·m^2, which partially restore the local symmetry between the monolayers. The large magnitude of s cannot represent the direct intermolecular interactions between peptides on opposite bilayer leaflets but rather indirect lipid mediated interactions, e. g. the formation of temporal nanopores between monolayers [47].

4. Conclusion

In the present study, we have conducted the first characterization of the material properties of GUVs at physiological buffer conditions. We have demonstrated that magainin 2 induces a substantial softening of POPC-bilayer vesicle reflected in the bending elastic modulus. The observed reduction in the bending stiffness is interpreted in terms of a continuum model involving coupling of peptides to membrane curvature, intra- and inter-monolayer peptide interactions, and information about model parameters are obtained from the experimental data. Our measurements and modeling leave a picture of magainins, inducing highly mobile regions with high curvature on the membrane surface, which soften the membrane and have some associations across the monolayers.

Acknowledgments

The authors would like to thank Torben Sørensen for the building of the chamber holder. This work was made possible due to a collaboration between MEMPHYS-Center for Membrane Biophysics, supported by the Danish National Research Foundation, and the UMR-CNRS 6510, supported by the Centre National de la Recherche Scientifique. This study was also financed by the French Embassy in Denmark.

References

[1] M. Zasloff, Magainins, a class of antimicrobial peptides from Xenopus skin: isolation, characterization of two active forms, and partial cDNA sequence of a precursor, Proc. Natl. Acad. Sci. U. S. A. 44 (1987) 5449–5453.
[2] M. Zasloff, B. Martin, H.C. Chen, Antimicrobial activity of synthetic magainin peptides and several analogues, Proc. Natl. Acad. Sci. U. S. A. 85 (1988) 910–913.
[3] K. Matsuzaki, Magainins as paradigm for the mode of action of pore forming polypeptides, Biochim. Biophys. Acta 1376 (1998) 391–400.
[4] T. Wieprecht, O. Apostolov, J. Seelig, Binding of the antibacterial peptide magainin 2 amide to small and large unilamellar vesicles, Biophys. Chemist. 85 (2000) 187–198.
[5] W.R. Williams, R. Starman, K. Taylor, K. Gable, T. Beeler, M. Zasloff, D. Covelle, Raman spectroscopy of synthetic antimicrobial frog peptide magainin 2a and PGLa, Biochemistry 29 (1990) 4490–4496.
[6] M. Jackson, H.H. Mantsch, J.H. Spence, Conformation of magainin-2 and related peptides in aqueous solution and membrane environments probed by Fourier transform infrared spectroscopy, Biochemistry 31 (1992) 7289–7293.
[7] T. Wieprecht, M. Dathe, M. Schümann, E. Krause, M. Beyermann, M. Bienert, Conformational and functional study of magainin 2 in model membrane environments using the new approach of systematic double-D-amino acid replacement, Biochemistry 35 (1996) 10844–10853.
[8] D. Marion, M. Zasloff, A. Bax, A two-dimensional NMR study of the antimicrobial peptide magainin 2, FEBS Lett. 227 (1998) 21–26.
[9] K. Matsuzaki, M. Harada, S. Funakoshi, N. Fujii, K. Miyajima, Physicochemical determinants for the interactions of magainins 1 and 2 with acidic lipid bilayers, Biochim. Biophys. Acta 1063 (1991) 162–170.
[10] B. Bechinger, Y. Kim, L.E. Chirlian, J. Gesell, J.M. Neumann, M. Montal, J. Tomich, M. Zasloff, S.J. Opella, Orientations of amphipatic helical peptides in membrane bilayers determined by solid-state NMR spectroscopy, J. Biomol. NMR 1 (1991) 167–173.
[11] B. Bechinger, M. Zasloff, S.J. Opella, Structure and interactions of magainin antibiotic peptides in lipid bilayers: a solid-state nuclear magnetic resonance investigation, Biophys. J. 62 (1992) 2–14.
[12] B. Bechinger, M. Zasloff, S.J. Opella, Structure and orientation of the antibiotic magainin in membranes by solid-state nuclear magnetic resonance spectroscopy, Protein Sci. 2 (1993) 2077–2084.
[13] M. Milik, J. Skolnick, Insertion of peptide chains into lipid membranes: an off-lattice Monte Carlo dynamics model, Proteins 15 (1993) 10–25.
[14] K. Matsuzaki, O. Murase, H. Tokuda, S. Funakoshi, N. Fujii, K. Miyajima, Orientational and aggregational states of magainin 2 in phospholipid bilayers, Biochemistry 33 (1994) 3342–3349.
[15] S.J. Ludtke, K. He, Y. Wu, H.W. Huang, Cooperative membrane insertion of magainin correlated with its cytolytic activity, Biochim. Biophys. Acta 1190 (1994) 181–184.
[16] M. Schümann, M. Dathe, T. Wieprecht, M. Beyermann, M. Bienert, The tendency of magainin to associate upon binding to phospholipid bilayers, Biochemistry 36 (1997) 4345–4351.
[17] S.J. Ludtke, K. He, H.W. Huang, Membrane thinning induced by magainin 2, Biochemistry 34 (1995) 16764–16769.
[18] H. Zhao, Mode of action of antimicrobial peptides, Thesis, University of Helsinki (2003).
[19] S.J. Ludtke, K. He, W.T. Heller, T.A. Harroun, L. Yang, H.W. Huang, Membrane pores induced by magainin, Biochemistry 35 (1996) 13723–13728.
[20] K. Matsuzaki, K. Sugishita, N. Ishibe, M. Ueha, S. Nakata, K. Miyajima, R.M. Epand, Relationship of membrane curvature to the formation of pores by magainin 2, Biochemistry 37 (1998) 11856–11863.
[21] M.S.P. Sansom, The biophysics of peptide models of ion channels, Prog. Biophys. Mol. Biol. 55 (1991) 139–235.
[22] B. Bechinger, Structure and functions of channel-forming polypeptides: magainins, cecropins, melittin and alamethicin, J. Membr. Biol. 156 (1997) 197–211.
[23] Y. Shai, Mechanism of binding, insertion and destabilization of phospholipid bilayer membranes by α-helical antimicrobial and cell non-selective lytic peptides, Biochim. Biophys. Acta 1462 (1999) 55–70.
[24] Z. Oren, Y. Shai, Mode of action of linear amphiphatic alpha-helical antimicrobial peptides, Biopolymers 47 (1998) 451–463.
[25] B. Bechinger, R. Kinder, M. Helmle, T.B. Vogt, U. Harzer, S. Schinzel, Peptide structural analysis by solid-state NMR spectroscopy, Biopolymers 51 (1999) 174–190.
[26] B. Bechinger, Detergent-like properties of magainin antibiotic peptides: a P^{31} solid-state NMR spectroscopy study, Biochim. Biophys. Acta 1712 (2005) 101–108.
[27] B. Bechinger, The structure, dynamics and orientation of antimicrobial peptides in membranes by multidimensional solid-state NMR spectroscopy, Biochim. Biophys. Acta 1462 (1999) 157–183.
[28] B. Bechinger, K. Lohner, Detergent-like actions of linear amphiphatic cationic antimicrobial peptides, Biochim. Biophys. Acta 1758 (2006) 1529–1539.
[29] M.I. Angelova, D.S. Dimitrov, Liposome electroformation, Faraday Discuss. Chem. Soc. 81 (1986) 303–311.
[30] M.I. Angelova, S. Soléau, P. Méléard, J.F. Faucon, P. Bothorel, Preparation of giant vesicles by external AC electric fields. Kinetics and applications, Prog. Colloid & Polym. Sci. 89 (1992) 127–131.
[31] T. Pott, H. Bouvrais, P. M, é l é ard, Giant unilamellar vesicle formation under physiological relevant conditions, Chem. Phys. Lipids (2008), doi:10.1016/j.chemphyslip.2008.03.008.
[32] W. Helfrich, Elastic properties of lipid bilayers: theory and possible experiments, Z. Naturforsch. 28 (1973) 693–703.
[33] J.F. Faucon, M. Mitov, P. M, é l é ard, I. Bivas, P. Bothorel, Bending elasticity and thermal fluctuations of lipid membranes. Theoretical and experimental requirements, J. Physique 50 (1989) 2389–2414.
[34] J.R. Henriksen, A. Rowat, J.H. Ipsen, Vesicle fluctuation analysis of the effects of sterols on membrane bending rigidity, Eur. Biophys. J. 33 (2004) 732–741.
[35] E. Evans, W. Rawicz, Entropy-driven tension and bending elasticity in condensed-fluid membranes, Phys. Rev. Lett. 64 (1990) 2094–2097.
[36] N. Kučerka, S. Tristram-Nagle, J.F. Nagle, Structure of fully hydrated fluid phase lipid bilayers with monounsaturated chains, J. Membr. Biol. 208 (2006) 193–202.
[37] J.R. Henriksen, J.H. Ipsen, Measurements of membrane elasticity by micropipette aspiration, Eur. Phys. J., E Soft Matter 14 (2004) 149–167.
[38] V. Vitkova, P. Méléard, T. Pott, I. Bivas, Alamethicin influence on the membrane bending elasticity, Eur. Biophys. J. 35 (2006) 281–285.

[39] C. Gerbeaud, Effet de l'insertion de protéines et de peptides membranaires sur les propriétés mécaniques et les changements morphologiques de vésicules géantes, Thèse, Université de Bordeaux I (1998).
[40] C. Li, T. Salditt, Structure of magainin and alamethicin in model membranes studied by X-Ray reflectivity, Biophys. J. 91 (2006) 3285–3300.
[41] G. Lantzsch, H. Binder, H. Heerklotz, Surface area per molecule in lipid/$C_{12}E_n$ membranes as seen by fluorescence resonance energy transfer, J. Fluoresc. 4 (1994) 339–343.
[42] T. Wieprecht, M. Beyermann, J. Seelig, Binding of antibacterial magainin peptides to electrically neutral membranes: thermodynamics and structure, Biochemistry 38 (1999) 10377–10387.
[43] J.A. Gazzara, M.C. Philipps, S. Lund-Katz, et al., Effect of vesicle size on their interaction with class A amphipatic helica peptides, J. Lipid Res. 38 (1997) 2147–2154.
[44] A. Zemel, A. Ben-Shaul, S. May, Perturbation of a lipid membrane by amphiphatic peptides and its role in pore formation, Eur. Biophys. J. 34 (2005) 230–242.
[45] A. Zemel, A. Ben-Shaul, S. May, Membrane perturbation induced by interfacially adsorbed peptides, Biophys. J. 86 (2004) 3607–3619.
[46] S. Leibler, Curvature instability in membranes, J. Physique 47 (1986) 507–516.
[47] H. Leontiadou, A.E. Mark, S.J. Marrink, Antimicrobial peptides in action, J. Am. Chem. Soc. 128 (2006) 12156–12161.